SUPPLEMENTAL MATERIALS

Variable Activation of the DNA Damage Response Pathways in Patients Undergoing SPECT Myocardial Perfusion Imaging

Won Hee Lee, PhD[1-3]*, Patricia Nguyen, MD[1-4]*, Shijun Hu, PhD[1,2], Grace Liang, BS[3,4], Sang-Ging Ong, PhD[1,2], Leng Han, PhD[1,2],Veronica Sanchez-Freire, PhD[2], Andrew S. Lee, PhD[2], Minal Vasanawala, MD[4], George Segall, MD[4], Joseph C. Wu, MD, PhD[1-3]

[1]Department of Medicine, Division of Cardiology, [2]Department of Radiology, Molecular Imaging Program, [3]Stanford Cardiovascular Institute, Stanford University School of Medicine, Stanford, CA, [4]Veterans Administration Palo Alto, Palo Alto, CA

*Contributed equally

SUPPLEMENTAL METHODS

In Vitro Irradiation and Culture

All irradiations were performed at room temperature. For measuring proteomic changes, we irradiated blood samples from healthy volunteers with a 800 Ci self-shielded ^{137}Cs γ-irradiator (J.L. Shepherd & Associates, San Fernando, CA) at an average dose rate of 1.38 Gy/min for low doses (e.g., 12.5, 25, or 50 mGy). Given that protein changes are short-lived but have been detected up to 5 hours after low dose radiation exposure,[1] we measured the changes in phosphorylation 2 hours after irradiation to assess the contribution of the initial SPECT dose on the overall phosphorylation. For gene expression analysis, we divided the total dose delivered (e.g., 25 mGy) into two fractions (1st irradiation: 25% of total dose versus 2nd irradiation: 75% of total dose 1.5 hours after 1st irradiation) in order to simulate doses administered to patients undergoing SPECT imaging. Control samples underwent sham irradiation. For incubation times longer than 30 minutes, blood samples were immediately diluted at a 1:1 ratio with RPMI 1640 medium (Mediatech Inc., Manassas, VA) containing 10% heat-inactivated fetal bovine serum after irradiation, returned to the CO_2 incubator, and maintained at 37°C in 5% CO_2/95% air until the appropriate time point for analysis.

Sample Preparation for T-lymphocyte Subpopulation

Freshly isolated PBMCs were pre-incubated with 20 µl of FcR-blocking reagent (Miltenyi) and labeled by addition of CD3-Alexa Fluor 647 (BD Biosciences), CD4-phycoerythrin (PE; BD Biosciences), CD62L-phycoerythrin-cyanin7 (PECy7; eBioscience), CD45RA-allophycocyanin 780 (APC780; eBioscience), CD19-Alexa Fluor 700 (eBioscience), CD11-brilliant violet 605 (BioLegend, San Diego, CA) for 20 minutes on ice. Dead cells were excluded by adding 7-AAD

to the cell suspension prior to sorting. Using a FACS Aria (BD Biosciences), two subpopulations for $CD3^{+}CD4^{+}$ and $CD3^{+}CD8^{+}$ T-lymphocytes including naïve ($CD62L^{+}CD45RA^{+}$; Naïve) and central memory ($CD62^{+}CD45RA^{-}$; CM) were sorted directly into 96 well 0.2 ml PCR plates for single cell quantitative real-time PCR.

SUPPLEMENTAL FIGURE LEGENDS

Supplemental Figure 1. The percentage of phosphorylated cells for DNA damage-marker proteins in T-lymphocytes after exposure to low dose irradiation *in vitro*. T-lymphocytes were isolated 2 hours post-irradiation (0, 12.5, 25, or 50 mGy). **(A)** Total and phospho-H2AX (γ-H2AX), **(B)** phospho-p53, and **(C)** phospho-ATM were measured by flow cytometry (n=4-8). Two-dimensional dot plots of the percentage of total and phospho-H2AX detected at each radiation dose are shown in the upper left hand corner. The numbers in the upper right area of each dot plot reflect the percentage of cells that express each surface marker. The numbers in the upper left hand corner reflect those that express only γH2AX (phosphorylated H2AX). Those in the upper right hand corner are cells that express both γH2AX and H2AX. Those in the lower left hand corner are cells that express neither γH2AX nor H2AX (i.e., debris). Finally, those in the lower right hand corner are cells that express only H2AX. Line graphs showing the percentage of cells expressing phosphorylated DNA damage markers are shown in the remaining panels. Each individual data point represents a separate patient sample before (closed circle) and after *in vitro* low dose irradiation (open circle). Closed squares shown are displayed as mean ± SEM for each group. *Statistically significant from baseline (Bonferroni-adjusted $P<0.05$).

Supplemental Figure 2. The percentage of phosphorylated cells for DNA damage-marker proteins and relative mRNA expression of DNA repair-related genes in T-lymphocytes isolated from patients undergoing invasive X-ray angiography **(A, C,** and **E)** and echocardiography **(B, D,** and **F)**. Total and phospho-H2AX (γ-H2AX), phospho-p53, and phospho-ATM at baseline, post-angiography **(A)**, and post-echocardiography **(B)** were measured by flow cytometry (n=12 and n=9, respectively). Data shown are mean ± SEM for each group. *Statistically significant

from baseline (Bonferroni-adjusted P<0.05). A scatter plot showing protein activation in individual patients post-angiography **(C)** and post-echocardiography **(D)** measured by flow cytometry. Relative mRNA expression levels of *Bax*, *Ddb2*, *Mdm2*, *Atf6, Tp53,* and *Bbc3* at 24 hours following diagnostic angiography **(E)** and at 24 hours or 48 hours following echocardiography **(F)** were determined by single cell quantitative real-time PCR (n=10 and n=11, respectively). Data shown are mean ± SEM for each group. *Statistically significant from baseline (Bonferroni-adjusted P<0.05).

Supplemental Figure 3. The relative mRNA expression level of selected DNA repair-related genes in T-lymphocytes after exposure to low dose irradiation *in vitro*. Whole blood samples were irradiated with either 0 or 25 mGy (e.g., delivered as divided doses). Samples were maintained for 0, 6, 24, and 48 hours post-irradiation and T-lymphocytes were then isolated. The relative mRNA expression levels of **(A)** *Bax*, **(B)** *Atf6*, **(C)** *Mdm2*, **(D)** *Polh*, **(E)** *Map4k4*, **(F)** *Ccng1*, **(G)** *Ddb2*, **(H)** *Tp53*, and **(I)** *Bbc3* in T-lymphocytes were determined by single cell quantitative real-time PCR. Data shown are mean ± SEM for each group (n=3).

Supplemental Figure 4. Relative mRNA expression levels of **(A)** *Bax*, **(B)** *Ddb2*, **(C)** *Mdm2*, **(D)** *Atf6,* **(E)** *Tp53*, and **(F)** *Bbc3* in T-lymphocytes isolated from 27 patients at serial timepoints (i.e., baseline, 2 hours, 6 hours, 24 hours, and 48 hours) post-SPECT MPI were determined by single cell quantitative real-time PCR. Each individual data point at each time point represents a separate patient sample before (closed circle) and after SPECT MPI (open circle). Closed squares shown are displayed as mean ± SEM for each group. The number of patients collected at each time point is indicated in the figure.

Supplemental Figure 5. Bar graphs depicting the percentage of patients with Down (≥ 1.5-fold decrease), Up (≥ 1.5-fold increase), and No change in mRNA gene expression levels of **(A)** *Bax*, **(B)** *Ddb2*, **(C)** *Mdm2*, **(D)** *Atf6*, **(E)** *Tp53*, and **(F)** *Bbc*3 at 24 and 48 hours post-SPECT MPI (n=49).

Supplemental Figure 6. Phosphorylated cells for DNA damage-marker proteins **(A-B)** and relative mRNA expression of DNA repair-related genes **(C-D)** in human T-lymphocytes collected from different age groups (young and middle aged) after exposure to *in vitro* fractionated low dose irradiation. Data shown are mean ± SEM for each group (n=3).

Supplemental Figure 7. Relative mRNA expression of DNA repair-related genes in T-lymphocyte subpopulations after exposure to *in vitro* fractionated low dose irradiation (25 mGy). Relative mRNA expression levels of **(A)** *Bax*, **(B)** *Ddb2*, **(C)** *Mdm2*, **(D)** *Atf6*, **(E)** *Tp53*, and **(F)** *Bbc*3 at 24 hours following irradiation were determined by single cell quantitative real-time PCR. Data shown are mean ± SEM for each group (n=3). *Statistically significant from baseline (Bonferroni-adjusted $P<0.05$).

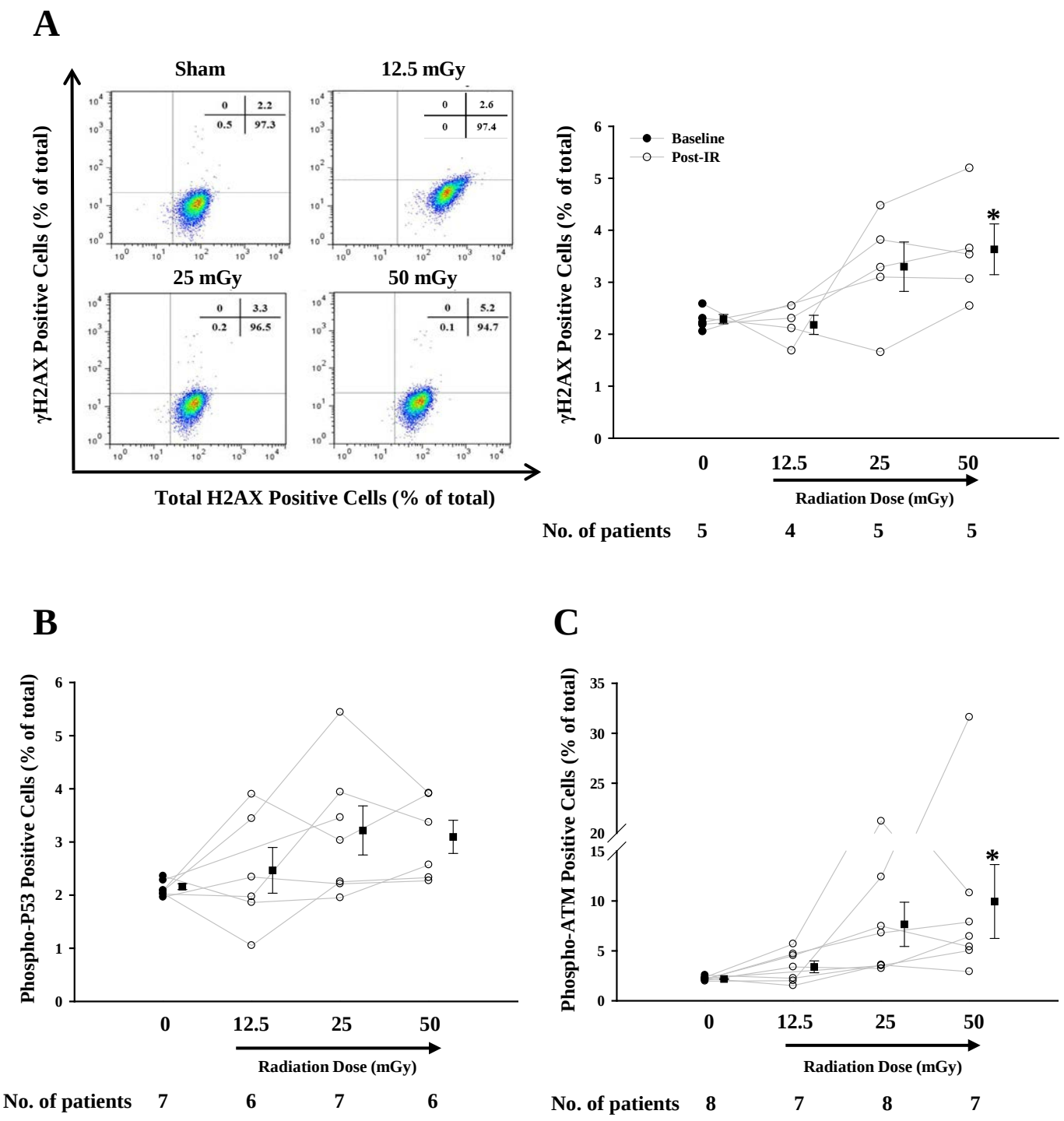

Supplemental Figure 1

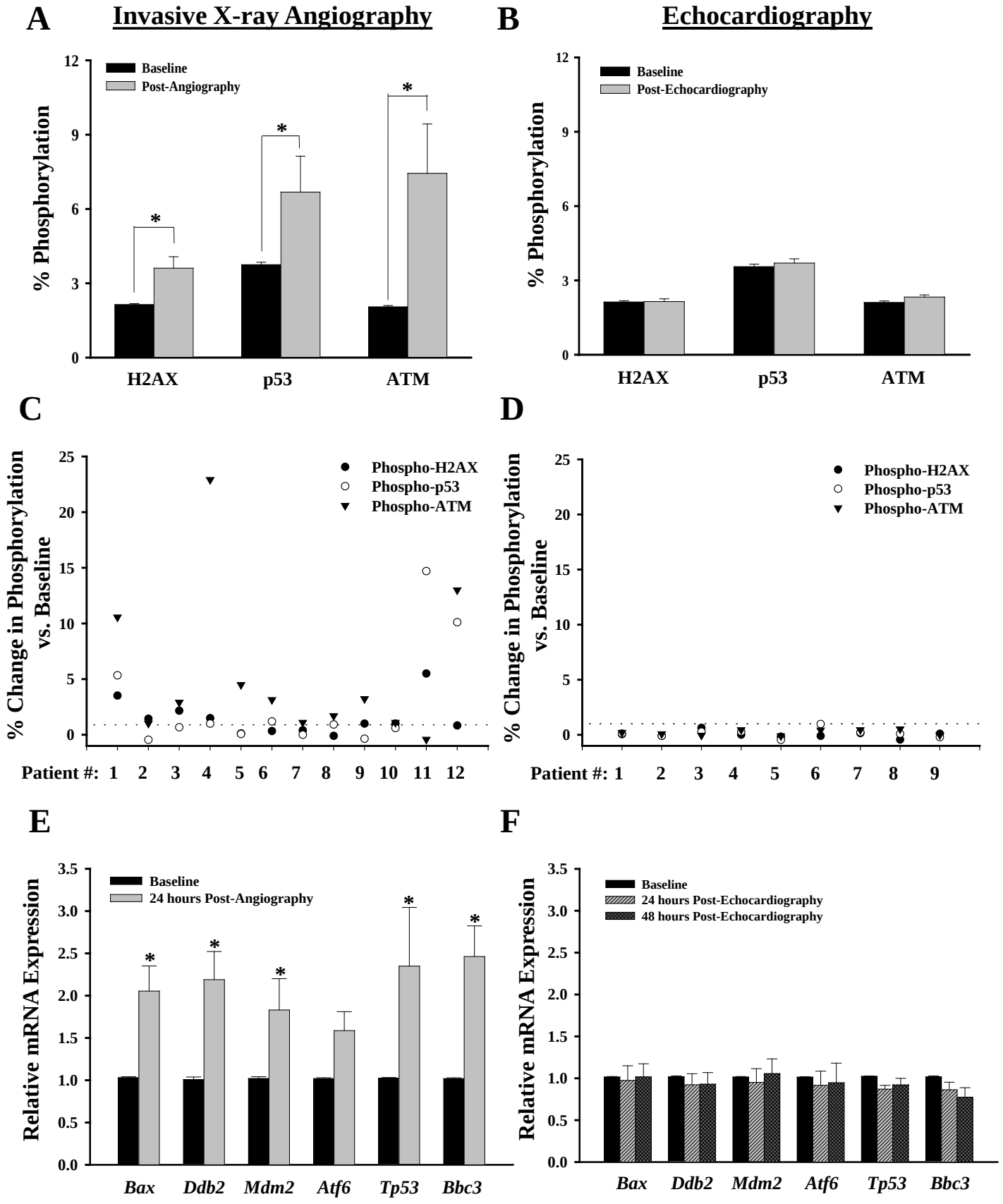

Supplemental Figure 2

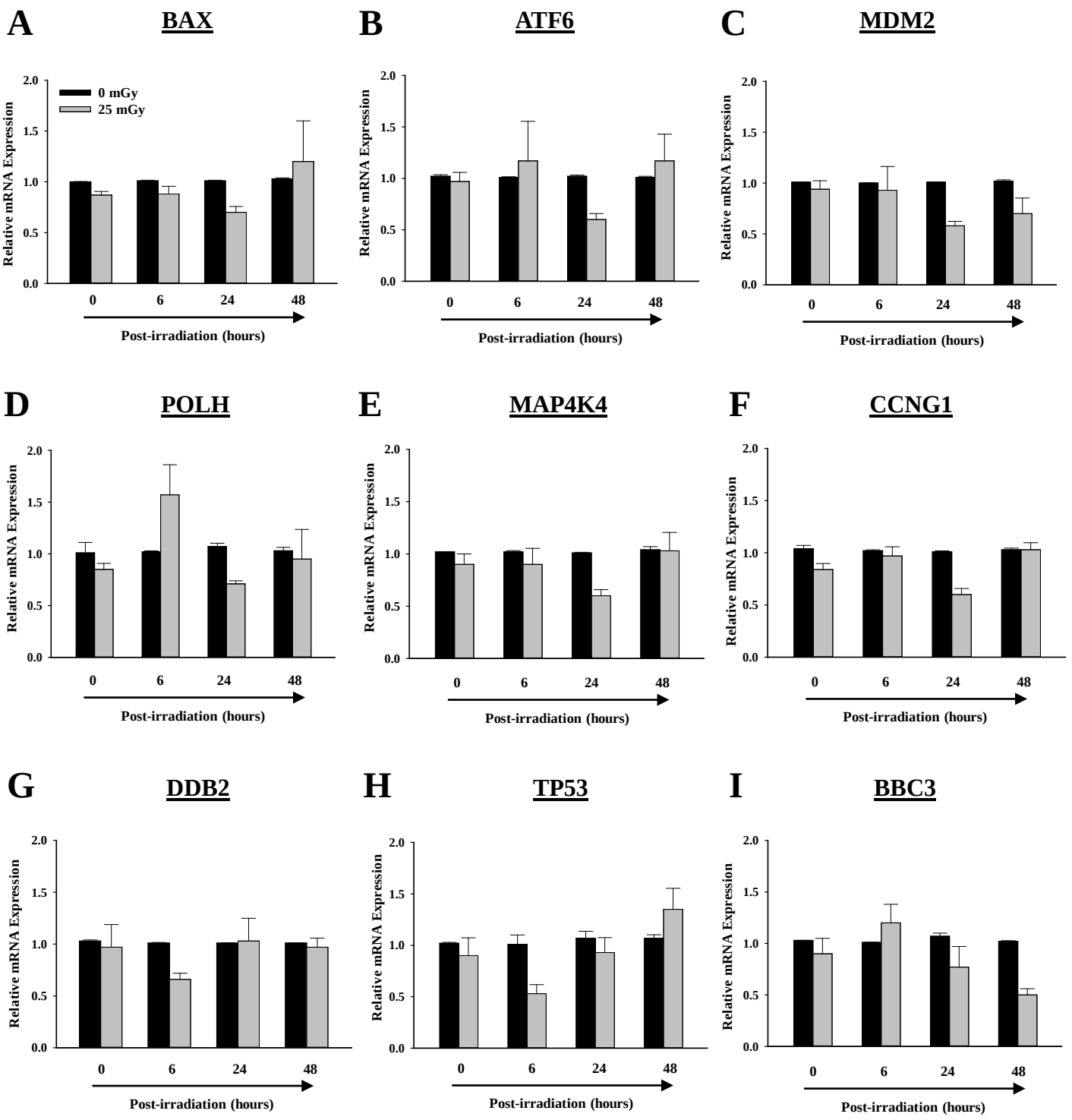

Supplemental Figure 3

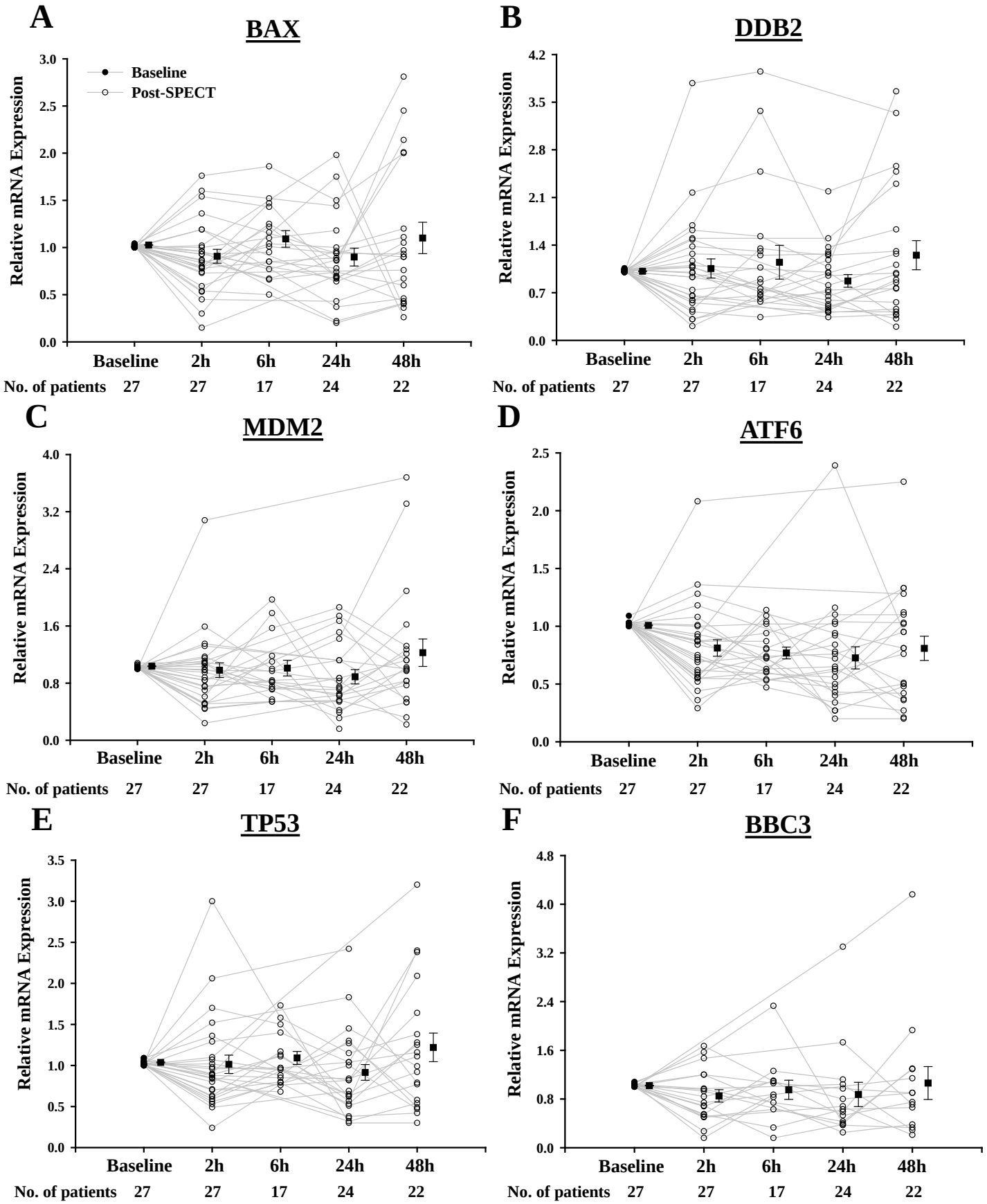

Supplemental Figure 4

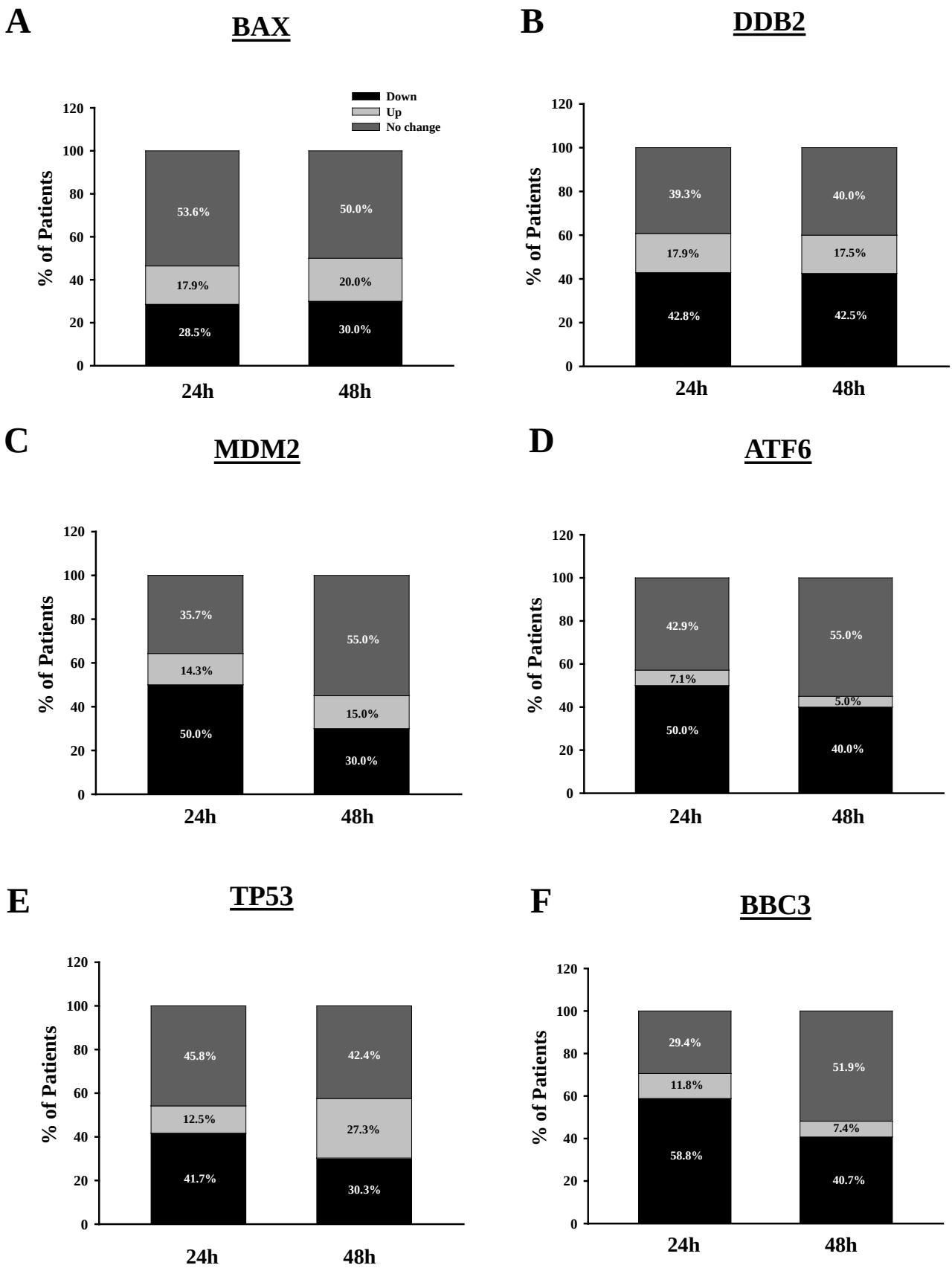

Supplemental Figure 5

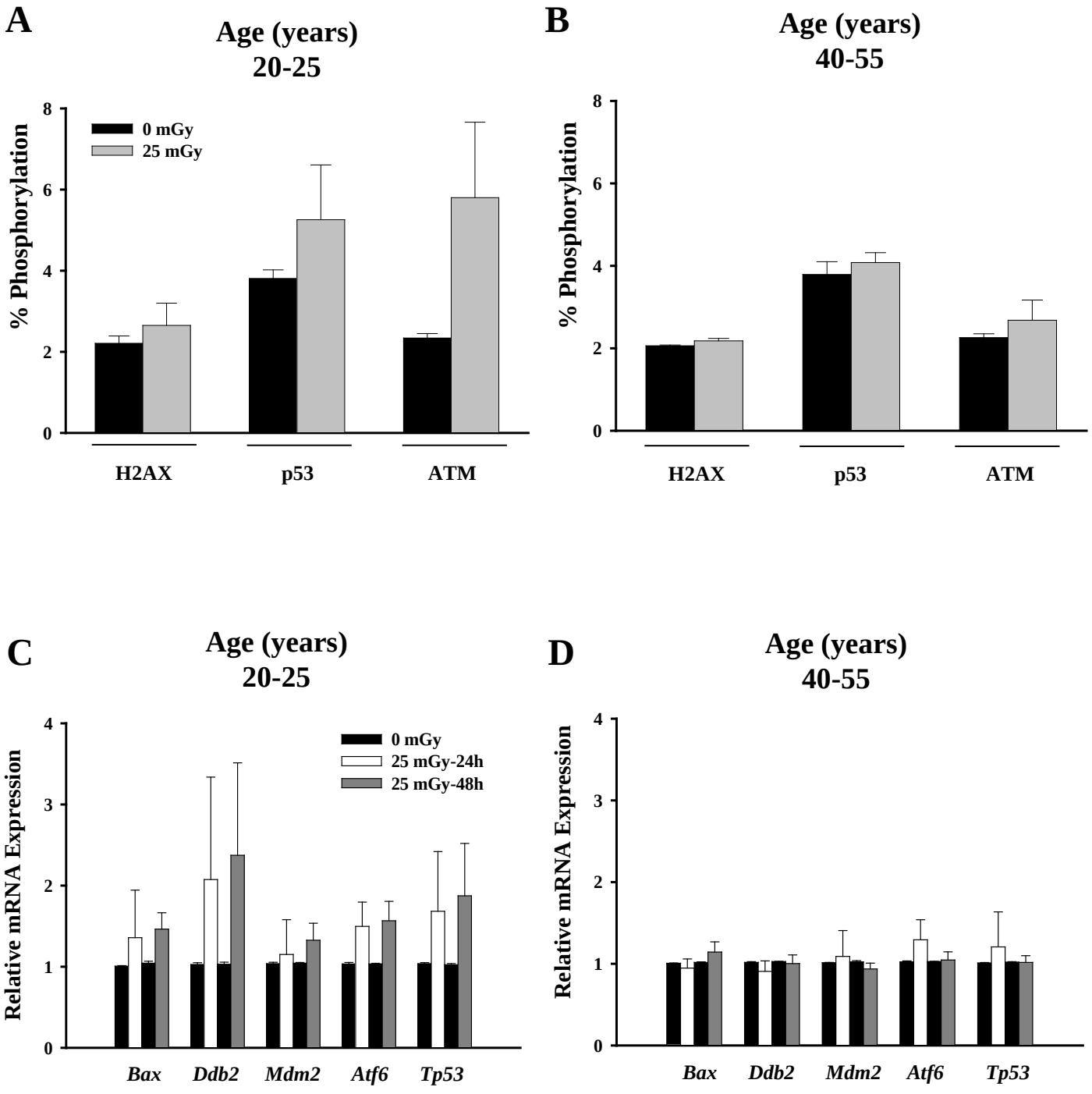

Supplemental Figure 6

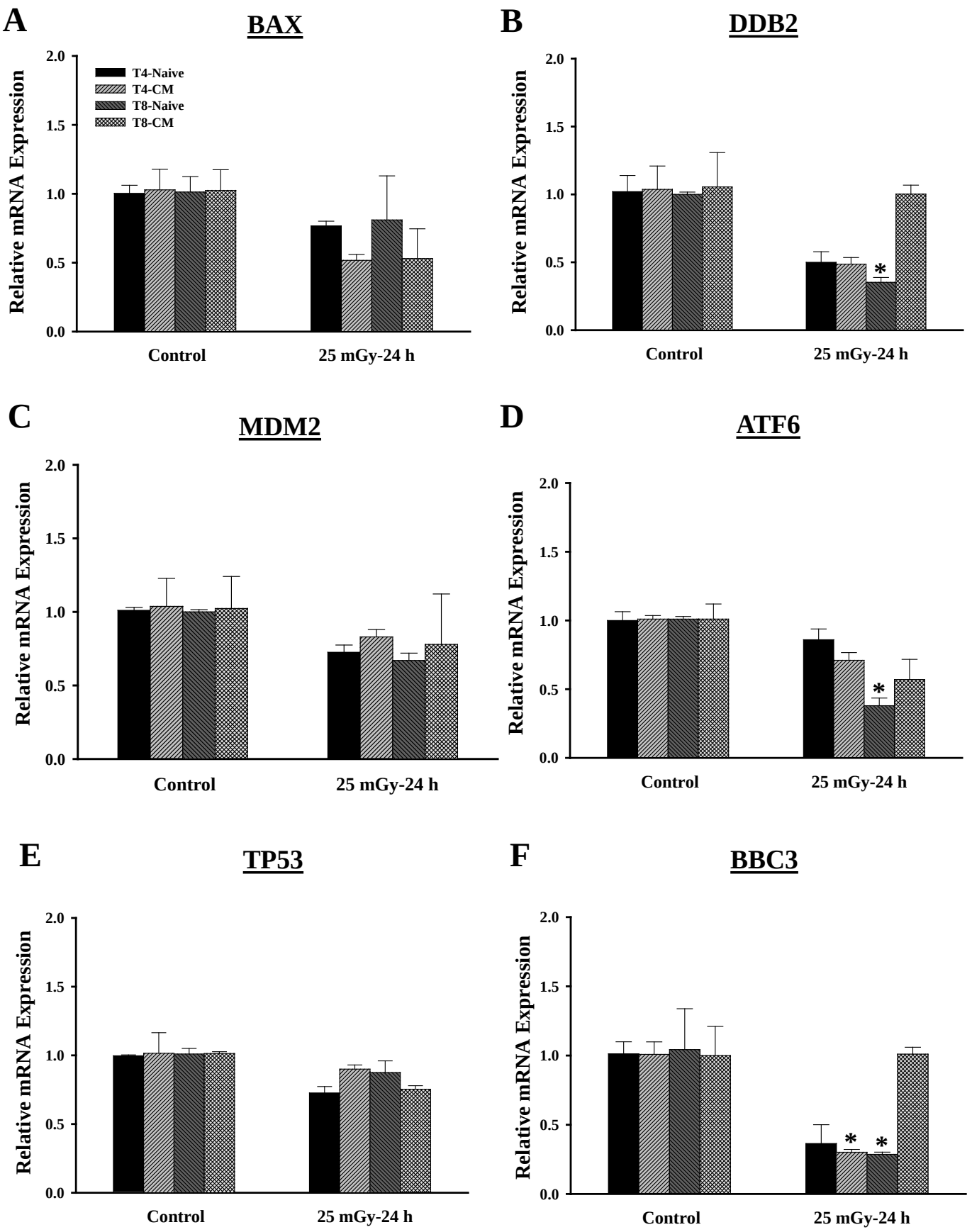

Supplemental Figure 7

Supplemental Table 1. Demographic and clinical characteristics of patients undergoing X-ray angiography (n=12) and echocardiography (n=15).

	Invasive X-ray Angiography	Echocardiography
Age (years)	63.7 ± 13.8	65.7 ± 17.3
Gender (%)		
Male	91.7	93.3
Female	8.3	6.7
Race (%)		
Caucasian	75	60
Clinical Factors		
Average BMI (kg/m^2)	32.4 ± 6.7	28.6 ± 4.6
History of Smoking (%)	75	73
History of Cancer (%)	8.3	13
Total Radiation Dose		
Total DAP ($cGy \cdot cm^2$)	7418±5287	N/A
Effective dose (mSv)	18.2±10.6	N/A

Data presented as mean ± SD or percentages. BMI, body mass index; kg, kilogram; mSv, millisievert; DAP, dose area product.

Supplemental Table 2. Genes selected for *in vitro* and *in vivo* gene expression analysis by single cell quantitative real-time PCR.

Gene Symbol	Description	Function
ATF6	Activating transcription factor 6	Apoptosis
BAX	Bcl-2-associated X protein	Apoptosis
BBC3	BCL2 binding component 3	Apoptosis
C12ORF5	Chromosome 12 open reading frame 5	Cell cycle
CCNG1	Cyclin G1	Cell cycle
CDK4	Cyclin-dependent kinase 4	Cell cycle
CDKN1A	Cyclin-dependent kinase inhibitor 1A	Cell cycle
DCLRE1C	DNA cross-link repair 1C	DNA repair
DDB2	Damage-specific DNA binding protein 2	DNA repair
FDXR	Ferredoxin reductase	Apoptosis
GADD45A	Growth arrest and DNA-damage-inducible, alpha	Cell cycle
JUN	Jun proto-oncogene	Cell cycle
MAP4K4	Mitogen-activated protein kinase kinase kinase kinase 4	Apoptosis
MDM2	Mdm2 p53 binding protein homolog	Cell cycle
PCNA	Proliferating cell nuclear antigen	DNA repair
POLH	Polymerase (DNA directed), eta	DNA repair
RAD 50	RAD 50 homolog	DNA repair
SESN1	Sestrin 1	Cell cycle
TP53 (P53)	Tumor protein p53	Apoptosis
XPA	Xeroderma pigmentosum, complementation group A	DNA repair
XPC	Xeroderma pigmentosum, complementation group C	DNA repair

Supplemental Table 3. Detection of DSBs in T-lymphocyte isolated from patients before and 30 minutes after SPECT by immunocytochemistry and flow cytometry (n=7).

	Microscopy of the # of γH2AX foci per T-lymphocyte			Flow cytometry of the % of γH2AX-positive T-lymphocytes		
	Baseline	Post-SPECT	P value	Baseline	Post-SPECT	P value
Mean ± SE	1.13 ± 0.05	1.47 ± 0.19	0.09	2.13 ± 0.07	2.31 ± 0.18	0.21
Median (MAD, IQR)	1.18 (0.10, 0.15)	1.38 (0.39, 0.68)		2.17 (0.13, 0.12)	2.36 (0.34, 0.48)	
MAD	0.10	0.39		0.13	0.34	
IQR	0.15	0.68		0.12	0.48	

Supplemental Table 4. The relative mRNA expression of DNA repair-related genes in T-lymphocytes isolated from 27 patients at different time points post-SPECT categorized as down (down, ≥1.5-fold decrease), up (up, ≥1.5-fold increase), and no change (noΔ).

ID	BAX				DDB2				MDM2				TP53				BBC3			
	2	6	24	48	2	6	24	48	2	6	24	48	2	6	24	48	2	6	24	48
A	no Δ	n/a	n/a	no Δ	up	n/a	n/a	up	no Δ	n/a	n/a	no Δ	n/a	n/a	n/a	n/a	no Δ	n/a	n/a	no Δ
B	down	n/a	down	down	down	n/a	down	no Δ	down	n/a	down	no Δ	no Δ	n/a	no Δ	up	no Δ	n/a	no Δ	down
C	down	no Δ	n/a	n/a	down	no Δ	n/a	n/a	no Δ	no Δ	n/a	n/a	down	no Δ	n/a	n/a	down	no Δ	n/a	n/a
D	no Δ	no Δ	n/a	n/a	no	no Δ	n/a	n/a	no Δ	down	n/a	n/a	no Δ	no Δ	n/a	n/a	no Δ	no Δ	n/a	n/a
E	no Δ	no Δ	no Δ	n/a	down	down	down	n/a	down	no Δ	no Δ	n/a	up	up	down	n/a	no Δ	down	down	n/a
F	no Δ	down	no Δ	n/a	down	down	no Δ	n/a	down	down	down	n/a	down	no Δ	down	n/a	down	no Δ	no Δ	n/a
G	no Δ	no Δ	no Δ	n/a	no Δ	no Δ	no Δ	n/a	no Δ	no Δ	no Δ	n/a	no Δ	no Δ	no Δ	n/a	down	no Δ	n/a	n/a
H	down	down	down	down	down	down	down	down	down	no Δ	down	down	no Δ	up	down	down	up	up	down	no Δ
I	no Δ	no Δ	no Δ	no Δ	up	up	no Δ	up	down	up	down	no Δ	down	no Δ	down	no Δ	up	no Δ	down	no Δ
J	no Δ	down	no Δ	down	no Δ	no Δ	down	no Δ	no Δ	no Δ	down	no Δ	up	up	no Δ	no Δ	up	up	up	up
K	no Δ	no Δ	no Δ	no Δ	no Δ	no Δ	no Δ	no Δ	down	down	down	no Δ	no Δ	no Δ	no Δ	no Δ	no Δ	no Δ	no Δ	no Δ
L	up	up	up	up	up	up	up	up	no Δ	up	up	no Δ	no Δ	no Δ	no Δ	no Δ	no Δ	no Δ	no Δ	no Δ
M	down	no Δ	no Δ	up	down	down	down	no Δ	no Δ	no Δ	down	no Δ	no Δ	no Δ	no Δ	no Δ	down	down	down	down
N	no Δ	no Δ	no Δ	no Δ	no Δ	no Δ	down	no Δ	up	no Δ	no Δ	up	no Δ	no Δ	no Δ	up	n/a	n/a	n/a	n/a
O	up	up	up	up	no Δ	no Δ	no Δ	up	no Δ	up	no Δ	up	no Δ	no Δ	down	up	down	down	down	no Δ
P	no Δ	no Δ	no Δ	up	up	up	no Δ	up	no Δ	no Δ	no Δ	up	no Δ	no Δ	no Δ	up	n/a	n/a	n/a	n/a
Q	no Δ	no Δ	no Δ	up	no Δ	down	no Δ	no Δ	no Δ	no Δ	down	no Δ	no Δ	no Δ	down	no Δ	n/a	n/a	n/a	n/a
R	no Δ	no Δ	no Δ	no Δ	down	no Δ	down	no Δ	no Δ	no Δ	no Δ	no Δ	no Δ	no Δ	down	no Δ	no Δ	no Δ	down	up
S	up	no Δ	up	up	up	up	up	up	up	up	up	up	up	up	up	up	n/a	n/a	n/a	n/a
T	no Δ	n/a	down	no Δ	no Δ	n/a	no Δ	no Δ	no Δ	n/a	down	no Δ	down	n/a	no Δ	down	n/a	n/a	n/a	n/a
U	no Δ	n/a	up	down	down	n/a	up	down	no Δ	n/a	up	down	up	n/a	up	no Δ	no Δ	n/a	up	no Δ
V	down	n/a	up	down	down	n/a	up	down	no Δ	n/a	no Δ	down	down	n/a	no Δ	down	down	n/a	no Δ	down
W	down	n/a	no Δ	down	down	n/a	down	no Δ	down	n/a	down	down	down	n/a	no Δ	down	n/a	n/a	n/a	n/a
X	no Δ	n/a	down	down	no Δ	n/a	down	down	no Δ	n/a	down	down	no Δ	n/a	down	down	no Δ	n/a	down	down
Y	no Δ	n/a	down	down	no Δ	n/a	down	down	no Δ	n/a	down	no Δ	no Δ	n/a	down	down	no Δ	n/a	down	down
Z	no Δ	n/a	down	down	no Δ	n/a	down	down	no Δ	n/a	no Δ	no Δ	up	n/a	up	n/a	n/a	n/a	n/a	n/a
Z1	no Δ	n/a	no Δ	no Δ	no Δ	n/a	no Δ	down	no Δ	n/a	no Δ	down	down	n/a	no Δ	n/a	n/a	n/a	n/a	n/a

SUPPLEMENTAL REFERENCES

1. Lobrich M, Rief N, Kuhne M, Heckmann M, Fleckenstein J, Rube C, Uder M. In vivo formation and repair of DNA double-strand breaks after computed tomography examinations. *Proc Natl Acad Sci U S A.* 2005;102:8984-8989.